Quantitative analysis of doped/undoped ZnO nanomaterials using laser assisted atom probe tomography: Influence of the analysis parameters

Nooshin Amirifar, Rodrigue Lardé, Etienne Talbot, Philippe Pareige, Lorenzo Rigutti, Lorenzo Mancini, Jonathan Houard, Celia Castro, Vincent Sallet, Emir Zehani, et al.

Quantitative analysis of doped/undoped ZnO nanomaterials using laser assisted atom probe tomography: Influence of the analysis parameters

Nooshin Amirifar,[1] Rodrigue Lardé,[1,a)] Etienne Talbot,[1] Philippe Pareige,[1] Lorenzo Rigutti,[1] Lorenzo Mancini,[1] Jonathan Houard,[1] Celia Castro,[1] Vincent Sallet,[2] Emir Zehani,[2] Said Hassani,[2] Corine Sartel,[2] Ahmed Ziani,[3] and Xavier Portier[3]

[1]*Groupe de Physique des Matériaux, UMR CNRS 6634, Université et INSA de Rouen, Avenue de l'Université, BP 12, 76801 Saint Etienne du Rouvray, France*

[2]*Groupe d'étude de la Matière Condensée (GEMAC), CNRS Université de Versailles St Quentin, 45 Avenue des Etats-Unis, 78035 Versailles Cedex, France*

[3]*Centre de Recherche sur les Ions, les Matériaux et la Photonique (CIMAP), UMR 6252 CEA-CNRS-ENSICAEN, Université de Caen, 14050 Caen, France*

(Received 15 June 2015; accepted 7 November 2015; published online 2 December 2015)

In the last decade, atom probe tomography has become a powerful tool to investigate semiconductor and insulator nanomaterials in microelectronics, spintronics, and optoelectronics. In this paper, we report an investigation of zinc oxide nanostructures using atom probe tomography. We observed that the chemical composition of zinc oxide is strongly dependent on the analysis parameters used for atom probe experiments. It was observed that at high laser pulse energies, the electric field at the specimen surface is strongly dependent on the crystallographic directions. This dependence leads to an inhomogeneous field evaporation of the surface atoms, resulting in unreliable measurements. We show that the laser pulse energy has to be well tuned to obtain reliable quantitative chemical composition measurements of undoped and doped ZnO nanomaterials. © *2015 AIP Publishing LLC*. [http://dx.doi.org/10.1063/1.4936167]

I. INTRODUCTION

In the last decade, zinc oxide (ZnO) has received a considerable attention due to its potential applications in optoelectronic, photonic, and electric devices. Wide and direct band gap (3.437 eV at 2 K) with large exciton binding energy (60 meV)[1,2] make ZnO a suitable candidate for fabrication of light emitting diodes at visible and UV range.[3–5] Moreover, ZnO can be easily synthesized in various nano-scale forms with low cost growth methods. However, the intrinsically n-type conductivity of ZnO has become a major obstacle in fabrication of p-type ZnO, and the origin of this behaviour has been a hot topic of many studies.[6,7] Phosphorous, nitrogen, arsenic, and antimony have been studied as possible acceptors.[2] Among all, nitrogen has been considered to be the best acceptor for p-type doping of ZnO as its similar ionic radius to the one of oxygen ion makes it replace oxygen sites more efficiently.[6] Several studies on nitrogen doped ZnO have also shown a successful fabrication of p-type ZnO.[3,8–10] Beside, ZnO doped with rare earth elements has attracted much attention in fabrication of light emitting diodes, since they provide good luminescent centers due to their narrow and intense emission lines originated from 4f intrashell transitions.[11] Many investigations have been performed on Eu and Tb doped ZnO since they are involved in the emission of red and green light, respectively.[12,13] However, finding a reliable method for synthesis of undoped and doped ZnO with a controlled dopant concentration is the main challenge in the development of ZnO based devices as the quality of the synthesized ZnO, concentration of the defects, and distribution of the dopants strongly affect its optical properties. Conventional techniques such as transmission electron microscopy (TEM), Photoluminescence (PL), Energy dispersive X-Ray spectroscopy (EDX), and secondary ion mass spectroscopy (SIMS) are commonly used in order to confirm the incorporation of the dopants in ZnO. However, these techniques are limited to the detection of only certain elements or up to certain concentrations which is often higher than the concentration of interest. Moreover, these techniques are often not applicable for variety of morphologies.

Laser assisted atom probe tomography (LA-APT) has appeared as a unique technique which is able to provide direct information about the chemical composition of elements together with a 3D map of position of each atom from a specimen at atomic scale. In the past, this technique was limited only to metallic material. Since 2006, thanks to the introduction of laser assisted atom probe,[14] it has become possible to perform APT analyses on semiconductors and insulating materials. In LA-APT, a laser pulse replaces the voltage pulse allowing for a controlled field evaporation of the atoms from the surface. The application of LA-APT technique was then significantly increased in order to investigate metallic, semiconductor and oxide nanomaterials such as magnetic multilayers,[15] transistors,[16] Si nanowires,[17] silicon-rich silica/silica multilayers,[18] and doped thin film semiconductors.[19]

Nevertheless, the physical phenomena behind laser-semiconductor interaction in LA-APT are not well understood as they are strongly influenced by the absorption properties of the semiconductor such as its band gap. Two main theories have been used to explain the field evaporation

[a)]Electronic mail: rodrigue.larde@univ-rouen.fr

mechanism in semiconductors: photo-ionization which involves the creation of the ions on the surface of the specimen, and then the evaporation of these ions.[20] This theory is applicable for materials with large band gap where the lifetime of the ions is long enough for the evaporation. Another theory is field evaporation through thermal mechanism. Once the specimen absorbs the laser energy, a localized heat occurs on the tip which assists in field evaporation by transferring energy to the surface atoms, and assisting them to overcome the potential barrier for ionization.[20] Recently, difficulties in quantitative APT measurements have been reported on semiconductors and oxides materials.[21,22] The laser parameters (wavelength, laser pulse energy, and continuous voltage) need to be properly adjusted in order to obtain the accurate chemical composition measurements.

We have observed in atom probe tomography analysis of ZnO that a small change in laser pulse energy (LPE) can strongly affect the overall composition of elements as well as the distribution of the atoms. The dependence of the composition on laser energy has been previously observed for $LiFePO_4$,[21] MgO,[22] CeO_2,[23] and GaN.[24–26]

To our knowledge, only few reports have been published on APT of ZnO where none has considered the optimum experimental condition for the experiment.[24,27,28]

The main purpose of this paper is to investigate the reliability of the APT measurements on ZnO material as a function of analysis parameters (laser wavelength and laser pulse energy) in order to achieve a proper condition for a reliable measurement. Having a good understanding of a proper condition for APT analysis, we address a quantitative study on incorporation of dopants for rare-earth doped ZnO thin films and nitrogen-doped ZnO nanowires.

II. EXPERIMENTAL DETAILS

In order to perform APT, the specimen should be prepared in the shape of a sharp needle with a tip radius of 50–100 nm. The basic operating principle of APT involves cooling the specimen down to $\leq$80 K in high vacuum. DC voltage in the range of 3–10 kV is applied that creates very high field strength at the tip. By applying additional high voltage or laser pulses, the atoms from the surface of the tip are then field evaporated and fly towards a position sensitive detector. The identity and composition of the atoms are then retrieved based on the mass spectra derived from the "time of flight" of each atom.

In APT of metallic materials, the laser light is absorbed by the free electrons, while in semiconductors, the electrons are bonded to the atoms. A laser wavelength corresponding to higher energy than the band gap energy can unbind these electrons and create free negative carriers in the conduction band and positive holes in the valence band. Thus, in case of ZnO, UV light ($\lambda = 343$ nm, $E_\lambda = 3.62$ eV) theoretically offers a better absorption. However, absorption can also be possible using wavelength corresponding to a lower energy than that of the band gap energy such as green light ($\lambda = 515$ nm, $E_\lambda = 2.41$ eV) by increasing the continuous voltage. In this case, the higher surface electric field yields a bandgap narrowing which increases the absorption of the semiconductor.[29]

In our study, we have thus investigated the influence of the laser wavelength on the APT measurements. Two laser modes were used: The UV mode with a wavelength $\lambda = 343$ nm and the green mode with a wavelength $\lambda = 515$ nm. For each mode, a systematic series of LPE was chosen to perform APT experiments. LPE was chosen between 0.5 nJ/pulse and 10 nJ/pulse for the UV mode and between 5 and 50nJ/pulse for the green mode. The spot size for UV and green mode is in the range of 20–40 μm and 15–30 μm, respectively. The APT experiments were also done on different undoped and doped ZnO nanomaterials (monocrystalline ZnO nanowires and polycrystalline ZnO thin films) in order to investigate the influence of the crystallinity. As the laser energy needed for evaporation is inversely related to the electric field, the lowest laser energy corresponds to the maximum field at the surface of the tip.

The undoped ZnO thin film was deposited by RF magnetron sputtering. Deposition was performed on a (100) silicon substrate heated at 100 °C. The total pressure and RF energy to target were fixed at 1.5 Pa and 1.91 W.cm^{-2}, respectively. Post-annealing treatments were carried out for 1 h under continuous nitrogen flow at a temperature of 500 °C. The doping of the thin films was performed by introducing calibrated europium oxide pellets on the surface of the ZnO target.

Undoped ZnO nanowires were grown on (0001) sapphire substrate in a horizontal MOCVD (Metal Organic Chemical Vapor Deposition) reactor working at low pressure (50 Torr). Diethylzinc (DEZn) and nitrous oxide (N_2O) were used as zinc and oxygen sources, and carrier gas was helium. The growth of the nanowires was carried out at 800 °C for 30 min. Nitrogen doped nanowires were obtained using the same process, and adding 15 cc/min of ammonia flow (NH_3) in the gas phase.

APT specimens of ZnO thin films were prepared using the lift-out method explained by Thompson *et al.*[30] In case of nanowires, APT specimen preparation is the main challenge particularly for the nanowires that are hardly visible under the optical microscope. In our work, the specimens were mainly prepared in several steps shown in Fig. 1. A single ZnO nanowire was mounted on top of a tungsten support tip under an optical microscope. The contact between the ZnO nanowire and the support tip was reinforced by a local Pt deposition using electron beam induced deposition (EBID).

For nanowires with a diameter larger than 100 nm, a small tip radius was obtained by annular milling at 30 kV and 1 pA using Zeiss N-Vision40 FIB-SEM focused ion beam.

All ZnO samples have been analysed by laser assisted wide-angle tomographic atom probe (LAWATAP, CAMECA) using femto-second laser pulses (350 fs) operating at a repetition frequency of 100 kHz. APT experiments were carried out at the fixed detection rate $\Phi = 2 \times 10^{-3}$ atoms/pulse with a working temperature of T = 40 K or T = 80 K. It is worth mentioning that during all the experiments, the applied continuous voltage (V_{dc}) was increased/decreased when the laser pulse energy was decreased/increased in order to maintain the

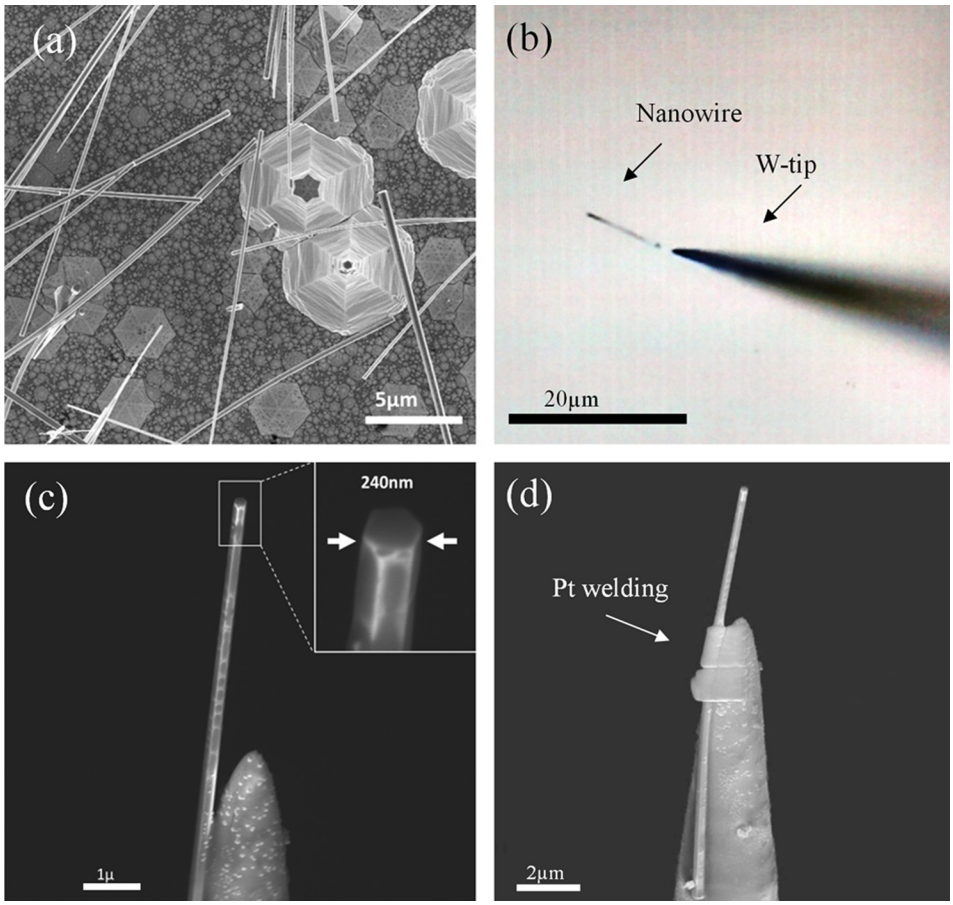

FIG. 1. APT specimen preparation of nanowires, (a) general view of ZnO nanowires, (b) mounting a nanowire (dispersed on a lam) on top of a W-tip under the optical microscope,(c) SEM image of the nanowire mounted on a W-tip, and (d) reinforcing the nanowire to the W-tip by EBID.

detection rate constant. Therefore, any laser energy variation is accompanied by a corresponding DC voltage variation.

In order to make a reliable comparison of the influence of different experimental conditions, dataset corresponding to different experimental parameters contains the same amount of collected atoms (200 000 atoms for each experiment).

Field ion microscopy (FIM), selected area electron diffraction (SAED), and HRTEM were also used to obtain information about the crystalline structure of the ZnO nanowires. To perform FIM, a mixture of Ne and He gas was used as the imaging gas at the pressure of 10^{-6} bar and the temperature of 80 K. Imaging was carried out using UV LPE of 0.1 nJ and a V_{dc} of 8 kV.

III. RESULTS AND DISCUSSION

A. Mass spectra

APT experiments were performed on undoped ZnO thin films and nanowires at different LPE in green and UV modes. Fig. 2 shows the effect of the LPE and laser wavelength on the mass spectra obtained for ZnO nanowire and thin film.

Figure 2(a) shows the mass spectrum obtained by APT on undoped ZnO nanowires with a LPE of 1nJ/pulse in UV mode. All the mass over charge ratio peaks can be identified to Zn, O, or molecular ions of both. The peak at 32 amu corresponds to an overlap of oxygen ($^{16}O_2^+$) and zinc ($^{64}Zn^{2+}$). The number of Zn and O ions in this peak can be obtained considering the natural isotopic abundance of Zn between 33 and 35 amu. There is also an uncertainty ascribing the peak at 16 amu that can be attributed to $^{16}O^+$, $^{16}O_2{}^{2+}$, or a mixture of both. The real nature of this peak is still under debate and has been identified as $^{16}O_2{}^{2+}$ by several authors[31–33] or $^{16}O^+$.[34] This problem can be solved by considering which assignment can provide an expected stoichiometry.[31]

For both nanowires and thin films specimens at lower laser pulse energies (Figs. 2(b) and 2(c)), the intensity of certain peaks such as Zn^+ at ~64 amu decreases. This loss in Zn^+ intensity is simultaneous with the increase in the Zn^{2+} amount, indicating the presence of a stronger electric field at the surface of the tip causing the post-ionization of the Zn atoms.[35] No significant difference has been observed between nanowires (Fig. 2(b)) and thin films (Fig. 2(c)). Moreover, at higher LPE, peaks corresponding to $Zn_3O_2{}^{2+}$ are revealed at around 112 amu (Figs 2(a) and 2(d)). These molecular ions commonly appear at higher LPE, because the field is not strong enough to avoid molecular evaporation. Furthermore, at lower LPE, the peak at 16 amu corresponding to oxygen becomes more important. Figs. 2(e) and 2(f) show the mass spectra obtained in green mode at low and higher LPE with the values of 10 nJ/pulse and 50 nJ/pulse, respectively. The same behavior, previously seen for UV mode, can be observed. For instance, increasing the LPE gives rise to an increase in the intensity of the peak at 32 amu. However, in green mode, this increase of the intensity appears less important as compared to the one of UV mode.

Comparing the mass spectra obtained in green and UV modes shows that the intensity of the peaks for the green

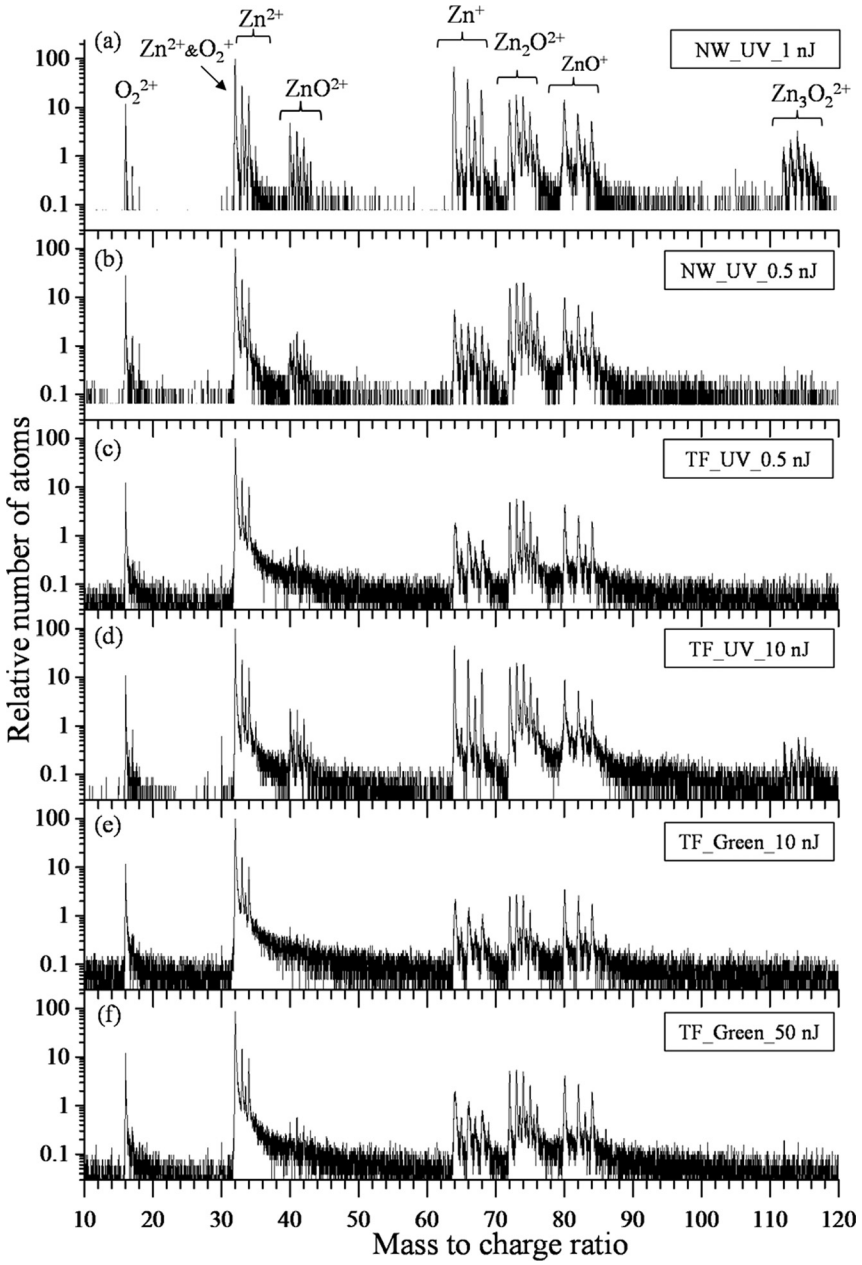

FIG. 2. Mass spectra for the relative number of atoms obtained by atom probe analysis of pure ZnO thin film (TF) and nanowire (NW) at different LPE using green and UV modes. Figure presents the mass spectra of ZnO nanowire using UV laser at (a) 1 nJ, (b) 0.5 nJ, ZnO thin film at (c) 0.5 nJ and (d) 10 nJ using UV laser, and ZnO thin film at (e) 10 nJ and (f) 50 nJ using green laser acquired at 80 K. The peak at 32 consists of both oxygen and zinc atoms, and the peak at 16 amu consists of pure O_2^+ or pure O^+ or a mixture of both.

mode exhibits the same behavior as the one obtained for smaller LPE using UV mode. However, the mass resolution (m/Δm) at full-width-half-maximum (FWHM) of the peaks does not vary significantly for different conditions. Table I shows the mass resolution of the peak at 32 amu corresponding to the mass spectra shown in Fig. 2. As it is presented in Table I, no significant difference can be observed in mass resolution of the peak 32 amu using green or UV laser modes.

TABLE I. The FWHM mass resolution of the peak at 32 amu corresponding to the mass spectra shown in Fig. 2.

Sample	*(a)*	*(b)*	*(c)*	*(d)*	*(e)*	*(f)*
ZnO	NW	NW	TF	TF	TF	TF
Mode	UV	UV	UV	UV	Green	Green
LPE (nJ/pulse)	1	0.5	0.5	10	10	50
m/Δm (FWHM)	400	533	457	640	457	400

The slightly lower resolution in green mode can be from the result of the deeper interaction with materials and the slower quenching using longer wavelength. It is worth to mention that in our experiment, APT of ZnO thin film with green laser at any laser energy shows a clear mass spectra which was not the case shown previously by Chen *et al.*[27]

As mentioned before, a higher electric field leads to post ionization of ions creating more doubly charged ions.[35] Therefore, the Zn^{2+}/Zn^+ ratio has been chosen as a reliable parameter to indirectly quantify the electric field strength and allowing us to compare APT experiments.[24] Such ratio is extracted from mass spectra (Fig. 2) by comparing intensities of Zn^{2+} and Zn^+ ions, respectively, in the 32–35 amu and 64–70 amu mass range values. Fig. 3 shows the evolution of the Zn^{2+}/Zn^+ ratio using UV and green modes at different LPE. For UV laser pulses, the Zn^{2+}/Zn^+ ratio is ranged from ~2.5 to ~4.5 and decreases monotonously with the increase in the LPE. This clearly indicates that the

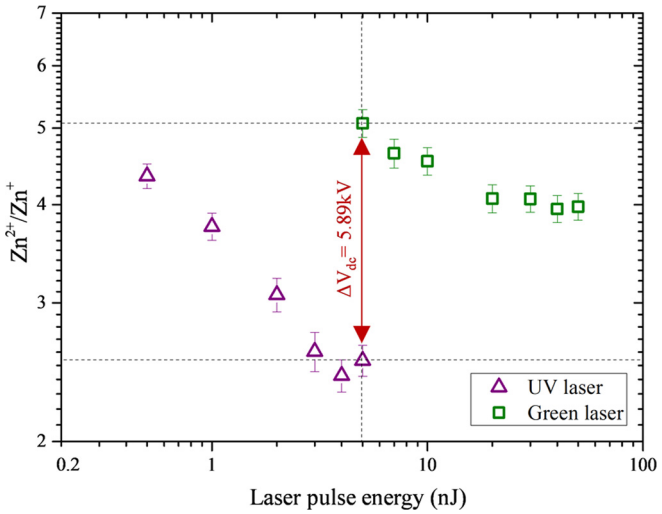

FIG. 3. The influence of LPE on Zn^{2+}/Zn^{+} ratio using UV and green modes. For the same LPE of 5 nJ, green mode provides higher ratio.

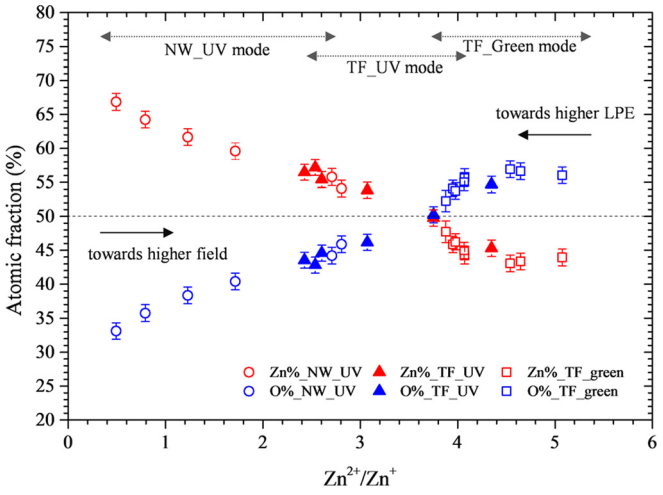

FIG. 4. The comparison of Zn (in red) and O (in blue) composition obtained by atom probe analysis for ZnO pure thin film (TF) using UV mode (solid triangle) and green mode (open square) and ZnO pure nanowires (open circle) at different LPE, as a function of charge state ratio representing the strength of the field on the tip.

increase in LPE leads to a decrease of the surface electric field at a constant detection rate. In this case, the decrease of the electric field is consistent with the observed decrease of the DC voltage.

In green mode, the Zn^{2+}/Zn^{+} ratio decreases slightly and it is ranged from ~4 to ~5. Green LPE provides a higher Zn^{2+}/Zn^{+} ratio than UV for the same LPE value, indicating the presence of a higher electric field on the surface of the tip. Considering a lower absorption of ZnO in green mode, a higher DC voltage is necessary in order to achieve the same detection rate as under UV illumination. This translates into a higher DC field and to an increase in Zn^{2+}/Zn^{+} ratio. In the present case, the difference in voltage is measured ΔV_{dc}=5.89 kV. It can be noted that the further increase or decrease of LPE is not possible in UV and Green modes.

Indeed, for both modes, if the LPE is too low, the continuous voltage becomes higher than the atom evaporation voltage resulting in an ungoverned field evaporation of atoms and a loss of chemical identification of the ions. If the LPE is too high, some laser ablation phenomena can be observed. From these results, we can conclude that using green mode cannot provide APT analysis at low electric field whereas the UV mode appears to be more versatile.

B. Chemical composition measurements

The atomic concentration of the elements can also be obtained simply by assigning each peak of the mass spectra to the corresponding ion and counting the number of atoms of each element associated to the peak.

Figure 4 shows the evolution of Zn and O concentrations as a function of Zn^{2+}/Zn^{+} ratio. The oxygen peak at 16 amu has been considered as O_2^{2+}. These measurements have been obtained for three cases: (a) ZnO thin film in UV mode, (b) ZnO thin film in green mode, and (c) ZnO nanowires in UV mode. The Zn^{2+}/Zn^{+} ratio has been tuned by changing the laser pulse energy (Fig. 3). We evidenced a continuous increase (decrease) of oxygen concentration (zinc concentration) with the increase of Zn^{2+}/Zn^{+} ratio from $X_O = 33\%$ ($X_{Zn} = 67\%$) to $X_O = 56\%$ ($X_{Zn} = 44\%$). Correct stoichiometric measurements can be achieved with a ratio of $Zn^{2+}/Zn^{+} \sim 3.8$.

This condition can only be obtained in UV mode. As mentioned previously, we cannot achieve this condition in green mode due to the continuous evaporation of atoms at very low green laser pulse energies. Moreover, in the same condition of UV LPE and mass to charge ratio, we observe the same behaviour on thin films and nanowires, indicating that sample morphology does not play a role in evaporation. Using the green mode provides the same trend as UV mode at first, followed by a stabilized value for zinc and oxygen atomic concentrations that is due to the stabilization of electric field mentioned previously (Fig. 3).

As it is clear in the figure, using UV mode and at Zn^{2+}/Zn^{+} ratio ranges from ~0.2 to ~3.8, the oxygen concentration is lower than the zinc concentration that can indicate a loss of oxygen atoms in the APT experiment. In green mode, for Zn^{2+}/Zn^{+} ratio ranges from ~4 to ~5, we observe the opposite behaviour that suggests a loss of zinc atoms. Our results indicate that in APT experiments of ZnO, the measured concentration is strongly dependent on the analysis parameters (laser wavelength, laser pulse energy, and continuous voltage).

Atomic concentrations of zinc and oxygen have been also calculated under the consideration of peak at 16 amu containing dominantly O^{+} ions. In this case, the corresponding Zn^{2+}/Zn^{+} value, at which the expected stoichiometry is measured, reduces only to 1%–5% lower than the one obtained previously. These results suggest that at this range of the field strength, assigning the peak at 16 amu to either O^{+} or O_2^{2+} amu does not modify the overall behavior of the measured fractions and yields only minor changes in measured composition. Therefore, in this work, the compositional information is carried out considering the peak at 16 amu contains only O_2^{2+} ions.

The loss of oxygen by the increase of LPE has been also evidenced in the literature. Santhanagopalan *et al.*[21] have

shown this effect on $LiFePO_4$ samples. They mentioned that an accurate measurement of oxygen content in green mode is possible but such condition does not provide reliable measurement of Li composition. The chemical compositions appeared to be more accurate in UV mode despite of some oxygen deficiency.

The dependence of chemical composition on LPE has also been previously observed for MgO,[22] CeO_2,[23] GaN,[26] and terbium doped ZnO thin film.[24] In all cases, the concentrations of the metallic element decreased while the concentration of non-metallic element increased by increasing the surface electric field (decreasing the LPE). In the case of MgO,[22] this behavior was addressed to the formation of holes localized on the oxygen corners of MgO lattice due to the laser irradiation. These holes were found to be responsible for the formation of oxygen and magnesium neutrals. The neutral species that are not field ionized would go undetected, and therefore, result in a loss of these elements. Since the field ionization potential of Mg is relatively less than O, it is less likely for desorbed neutral oxygen atoms to be field ionized at lower field. For GaN,[26] the field evaporation of c-axis GaN nanowire is found to be influenced by the formation of N_2 dimers. At high laser energies, sublimation of N_2 leads to the highly Ga-rich measurements.

In case of zinc oxide, one possible reason can be the difference in field ionization potentials of zinc (~9.39 eV (Ref. 36)) and oxygen (~13.61 eV (Ref. 22)). At high laser pulse energies, the surface electric field is strong enough to ionize only zinc atoms and not oxygen atoms leading to the oxygen deficiency. This is in agreement with the recent work of Xia *et al.*,[38] which show by first-principles calculation approach that Zn atoms are first evaporated. It is suggested that the Zn evaporation leads to an O enrichment. O atoms can then diffuse on the surface tip and thermal desorbed by the high laser energy resulting in neutral O atoms not detected by APT. At lower laser pulse energies, we suggest that the surface electric field is strong enough to ionize oxygen atoms (and/or oxygen molecules) that can lead to the increase in field evaporation efficiency of oxygen. Moreover, very high field (very low LPE) can cause continuous ionization and evaporation of zinc atoms between and after pulses that could not be detected leading to a Zn deficiency. This behavior is not observed in the Xia's theoretical work, because it is related to the detection method of ions in APT experiments.

C. APT analysis of doped ZnO materials

The results obtained previously for undoped ZnO have evidenced how variation of laser pulse energy and wavelength can significantly deviate the composition of elements from the stoichiometric value. Therefore, APT experiments on doped ZnO with an improper LPE can result in a bias on the concentration of the zinc, oxygen, and consequently, the dopant. Therefore, we found it crucial to investigate the influence of LPE on dopant concentration of doped ZnO materials. Two different ZnO doped nanostructures were chosen: europium doped ZnO thin films and nitrogen doped ZnO nanowires.

Figure 5 presents Eu and N dopant concentration as a function of Zn^{2+}/Zn^{+} ratio, where all measurements were carried out at constant evaporation rate using UV mode.

We can observe that Eu concentration decreases with the increase in surface electric field (decrease in LPE) as it was previously observed for Zn. However, the concentration of N increases by increasing the field (decreasing the LPE) as seen previously for oxygen.

The N-rich measurement at high field has been observed previously.[25] However, in most of the systems such as GaN, MgO, ZnO, and CeO, the lower field yields a cation-rich measurement and higher field results in anion-rich measurements. We have realized that the similar behavior of these elements can be associated with their similarity in their electronegativity value and their ability of losing electrons. For most of lanthanides, the electronegativity is of the order ~1.2 which is close to the electronegativity of Zn (1.65) while the electronegativity of O and N are 3.44 and 3.04, respectively.[37] The same conclusion can be made for the systems discussed previously, as Ga, Mg, and Ce show similar electronegativity values of 1.81, 1.31, and 1.12, respectively,[37] exhibiting the same concentration trend as a function of surface electric field. It is worth mentioning that regardless of the morphology of the tip and the APT condition for these two samples, the stoichiometric value for Zn/O

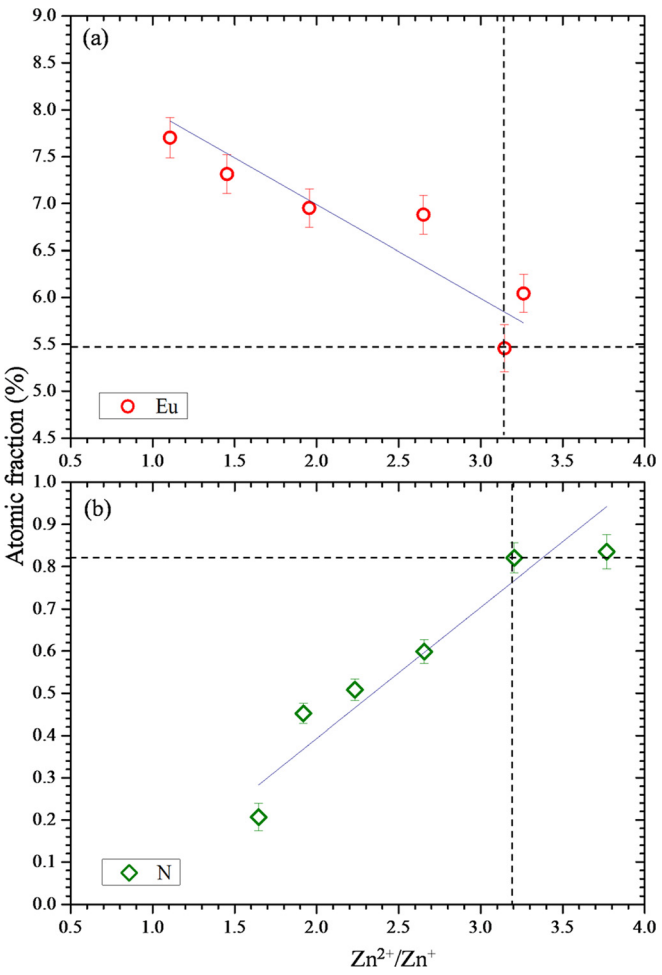

FIG. 5. Atomic composition of two doped samples: (a) Eu doped ZnO thin film and (b) nitrogen doped ZnO nanowire.

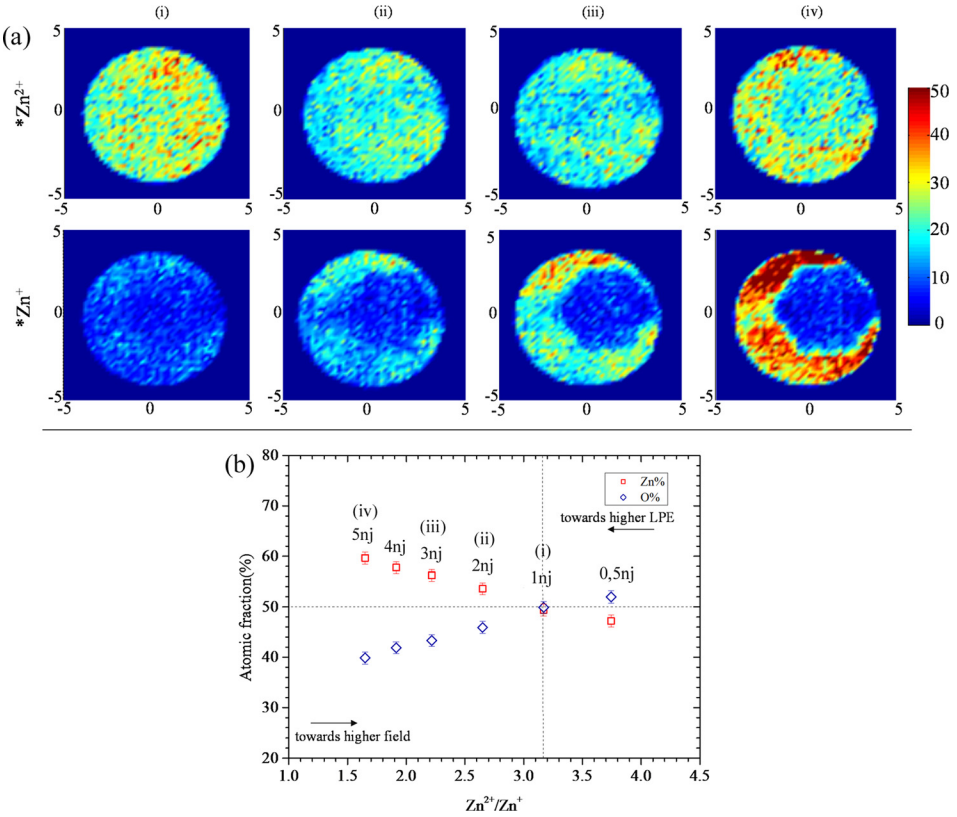

FIG. 6. APT of nitrogen doped ZnO single nanowire using UV laser. (a) Hitmap of the detected $*Zn^{+}$ and $*Zn^{2+}$ at the condition described in Table II where increasing the laser pulse energy results in a non-uniform detection of the elements. The star indicates that the Zn atoms corresponding to the major isotopic peak are excluded, (b) atomic fraction of zinc and oxygen obtained at each LPE as a function of charge state ratio. The stoichiometric ratio for Zn/O was obtained at the LPE of 1 nJ referring to the charge-state-ratio of about 3.2.

was obtained at almost the same value of Zn^{2+}/Zn^{+} which indicates the importance of laser pulse energy and the resulting surface electric field.

These results can bring confusion about the accurate concentration of the ZnO elements and dopants due to the strong dependence of concentration on the APT parameters. Nevertheless, we have observed that strong deviation of concentration occurs only at high laser energies where the surface electric field and field evaporation are not uniform, as it will be shown in the following. Hence, we suggest that the condition that provides Zn and O concentration close to the stoichiometric ratio of Zn/O can be assigned to the correct measurements and dopant concentration referring to this condition could be considered as the most appropriate value. For Eu and N doped ZnO, the stoichiometric ratio of Zn/O value is achieved at the Zn^{2+}/Zn^{+} ratio of 3.26 and 3.12 resulting in the Eu and N atomic concentration of about 6% and 0.8%, respectively. EDX measurements were performed on the Eu-doped ZnO thin film showing a measured Eu concentration ($5.5\% \pm 1\%$) very close to the concentration measured by APT. For N-doped ZnO nanowires, EDX is not suitable, and SIMS measurements are very difficult on a single nano-object but we can reasonably think that the N concentration value obtained by APT is close to the reality.

The presence of a non-uniform distribution of the surface electric field and ungoverned evaporation is confirmed by plotting the charge state hitmap of Zn at different LPE shown in Fig. 6(a). Such hitmap is used as an indicator of the distribution of electric field at the surface of the tip. The relative LPE and V_{dc} are presented in Table II. Since the peak at 32 amu contains both oxygen and zinc ions, for a more precise comparison, the peaks related to the maximum zinc isotope at 32 and 64 amu are excluded and not shown in the hitmaps. Following the hitmaps at different LPE, it is clear that the increase of LPE from 0.5 nJ to 5 nJ strongly affects the distribution of Zn^{+}. At lower LPE, the distribution of Zn^{+} is homogenous whereas at higher LPE the distribution becomes more and more inhomogeneous with a lower detection of Zn^{+} in a zone forming a clear hexagonal shape. Nevertheless, the distribution of Zn^{2+} is not affected by the LPE. Fig. 6(b) shows the Zn and O atomic fractions measured at different LPE of 0.5, 1, 2, 3, 4, and 5 nJ. The same evolution of Zn and O concentration as a function of charge state ratio can be observed as it was seen previously. The stoichiometric value is obtained for a Zn^{2+}/Zn^{+} ratio of 3.2 (LPE = 1nJ), where both Zn^{+} and Zn^{2+} ions are homogeneously distributed.

This result shows that increasing the LPE (decreasing the V_{dc} at constant detection rate) leads to an inhomogeneous distribution of the surface electric field. However, in order to investigate the origin of the particular field distribution at high LPE, a quantitative study has been carried out for the APT analysis at 5 nJ. Fig. 7(a) shows the distribution of Zn^{+} ions collected at LPE of 5 nJ, exhibiting a detection loss of Zn^{+} ions in a hexagonal region. This particular distribution

TABLE II. APT conditions attributed to Fig. 6 present the laser pulse energy, the corresponding V_{dc}, and the Zn^{2+}/Zn^{+} ratio.

	(i)	(ii)	(iii)	(iv)
LPE (nJ/pulse)	1	2	3	5
V_{dc} (kV)	6.75	6.18	5.8	5.27
Zn^{2+}/Zn^{+}	3.2	2.65	2.2	1.65

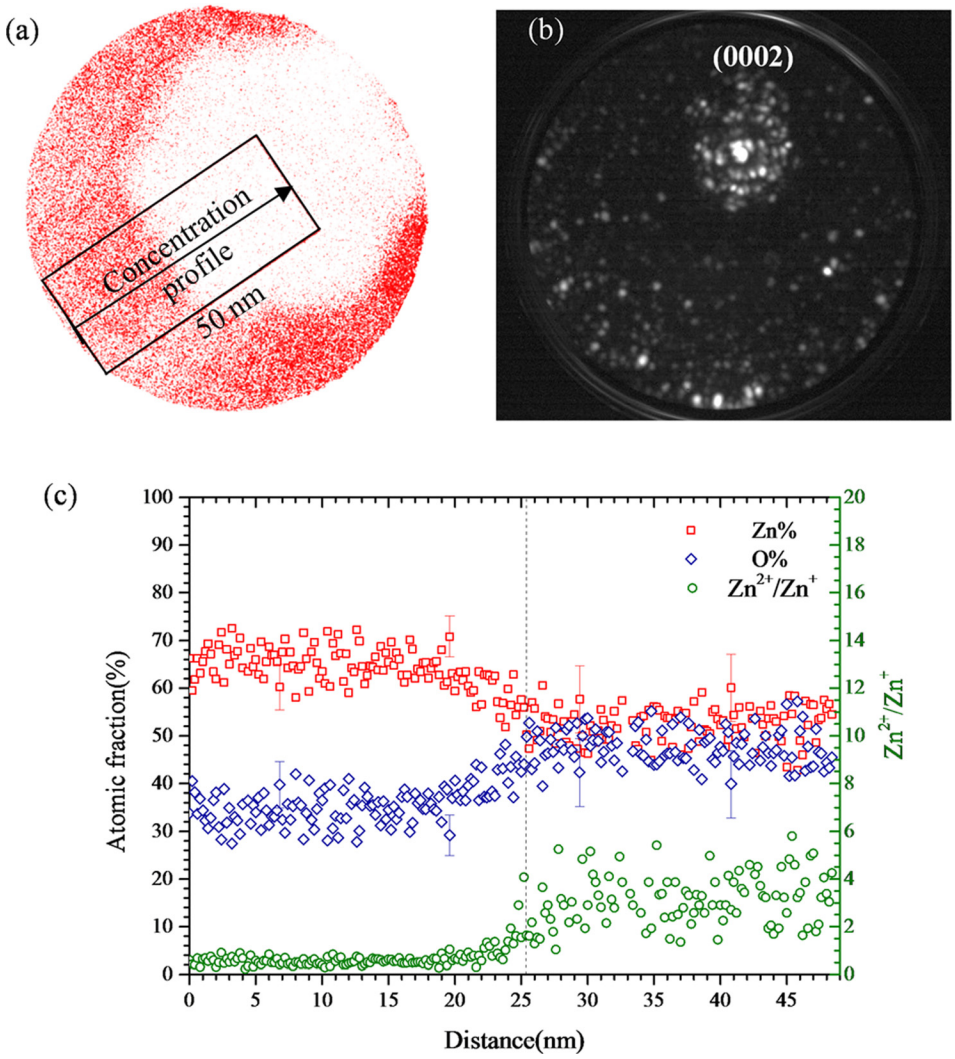

FIG. 7. (a) Distribution of Zn^{+} ions at LPE = 5 nJ, (b) field ion microscopy image of the same nanowire presenting the existence of a crystallographic pole at the place where the highest field is seen (c) concentration profile for a 3D selected zone shown in (a). For clarity reason, only few error bars are shown.

of Zn^{+} ions reflects the presence of a non-uniform distribution of the surface electrical field at this LPE. Fig. 7(b) shows the field ion microscopy image of the same specimen exhibiting a crystallographic pole at the place where a hexagon is observed in APT reconstructed volume. Hence, it brings the interest to investigate the local concentration of the elements in and out of the hexagonal region. Fig. 7(c) presents composition profile of Zn and O measured in the box indicated in Fig. 7(a). It was observed that the field is strongly increased in the hexagonal zone and where out of this zone, the field appeared at a very low value of Zn^{2+}/Zn^{+}. Hence, this strong difference in surface electric field results in the Zn/O ratio of about 70/30 at the low surface electric field region, evolving to almost 50/50 in the core region. Inside the hexagon region, the electric field is the highest and the measured Zn^{2+}/Zn^{+} is close to the one observed for LPE = 1 nJ. Inhomogeneity in the electric field at the surface leads then to a bias in the global composition measurements. However, this inhomogeneity of the surface electric field was not clearly observed on the ZnO thin films. In order to well understand these phenomena on ZnO nanowires, further investigations in HRTEM and SAED diffraction were performed on a single nanowire of the same sample (shown in Fig. 8). Fig. 8 shows that nanowire is well single crystallized in the wurtzite structure with a growth axis (0002).

The FIM image (Fig. 7(b)) confirms the orientation of the nanowires during the APT analysis. It can be noted that the observed pole corresponds to the highest electric field region of the entire FIM image. We can then conclude that the hexagonal area (the highest electric field region observed in APT) is correlated to the (0002) crystallographic direction of ZnO. These results may suggest that the distribution of the electric field at the tip surface is dependent on the

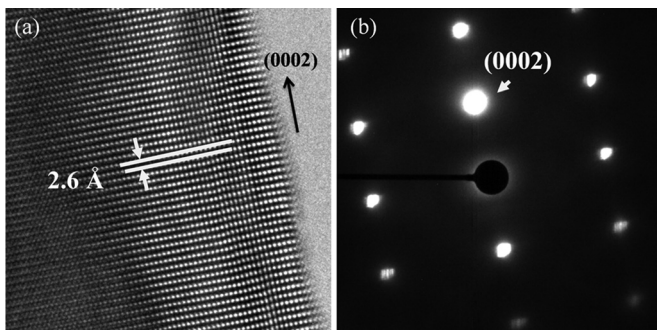

FIG. 8. (a) HTREM and (b) diffraction pattern in zone axis [01-10] of nitrogen doped ZnO nanowire, indicating the preferential growth along c-axis.

crystallographic direction. Moreover, this dependence becomes accentuated at higher LPE.

Finally, a series of N-doped ZnO nanowires was analyzed by APT using the suggested optimal condition of evaporation (LPE = 1nj, $Zn^{2+}/Zn^{+} \approx 3.2$). Figure 9 presents the obtained 3D reconstruction.

Statistical data treatments were performed from these data sets and show that for all analyzed samples, N atoms are distributed following a Poisson law which indicates that the distribution of N atoms is homogeneous in all the analyzed volume. Moreover, the N atomic concentration was measured around 0.8% for each sample. It shows that Zn^{2+}/Zn^{+} metric allows to perform reproducible experiments and should allow to follow the evolution of dopant concentration in a study of a series of nanowires grown at different dopant content.

IV. CONCLUSION

In this paper, we have investigated doped/undoped ZnO nanomaterials using APT. We have shown that the measured concentrations of oxygen and zinc are strongly dependent on the analysis parameters (laser wavelength, laser pulse energy, and continuous voltage). For both green and UV modes ($\lambda = 515$ nm and $\lambda = 343$ nm), at fixed evaporation flux, the variation of the LPE leads to the variation of the surface electric field expressed by the Zn^{2+}/Zn^{+} ratio. This parameter which is accurately measurable in APT experiment was chosen as the pertinent parameter to correlate the variation of the LPE and V_{dc} to the variation of the surface electric field. We have suggested that APT analyses are the most quantitative as possible for a range of surface electric field corresponding to a Zn^{2+}/Zn^{+} ratio around 3.5 in both UV and green mode. In green mode, the field evaporation of ZnO materials is possible. Nevertheless, the V_{dc} has to be strongly increased (as compared to the UV mode) leading to a high surface electric field.

It was observed that increasing the laser pulse energy creates a lower field on the tip and leads to zinc-rich measurements, whereas higher laser pulse energy results in oxygen rich-measurements. The reason behind this behaviour is yet ambiguous. However, Xia *et al*. work allows a better understanding. We can assume that at high LPE Zn atoms are first evaporated whereas O atoms diffuse and desorb, due to the thermal effect of the laser illumination leading to the formation of neutral oxygen which cannot be detected. It results in the high oxygen deficiency observed for Zn^{2+}/Zn^{+} ratio less than 3. By increasing the field (decreasing LPE), more oxygen atoms are ionized leading to a higher concentration of oxygen. Moreover, at higher field, the zinc atoms can evaporate between or after pulses causing lower detection of zinc atoms. Note that this behaviour at very high field (Zn^{2+}/Zn^{+} ratio more than 4) is not described in the work of Xia *et al*.[38]

The same variations in concentration have been also observed for Eu and N-doped ZnO nanomaterials. Concentration of Eu dopants was decreased by the increase in the field as it was seen previously for Zn. Nitrogen dopants, on the other hand, showed the same behaviour as oxygen where, by increasing the field, the concentration of the nitrogen increased. We have also observed, in N-doped ZnO nanowires, that the crystallographic orientation plays an important role on field evaporation of Zn^{+} ion at high LPE resulting in the deviation from stoichiometric condition. Indeed, for high LPE, inhomogeneous surface distribution of the electric field is observed. This phenomenon can be attributed to the faceting of the surface of the single crystal constituting the tip. In the low electric field region, a strong O deficiency was observed whereas in the high electric field region (0002 direction) the Zn/O ratio is close to 1.

This behaviour concerning the field distribution at the tip surface was not clearly observed in ZnO thin films due the nano-sized grains constituting the film (polycrystallinity).

In the light of the above observations, we can assume that the most appropriate condition to analyzed ZnO materials by atom probe tomography is defined for Zn^{2+}/Zn^{+} ratio around 3.5. Indeed in this range Zn^{2+}/Zn^{+} ratio, the field distribution is homogenous on the surface tip, and the Zn/O ratio is close to 1. It seems reasonable to postulate that this

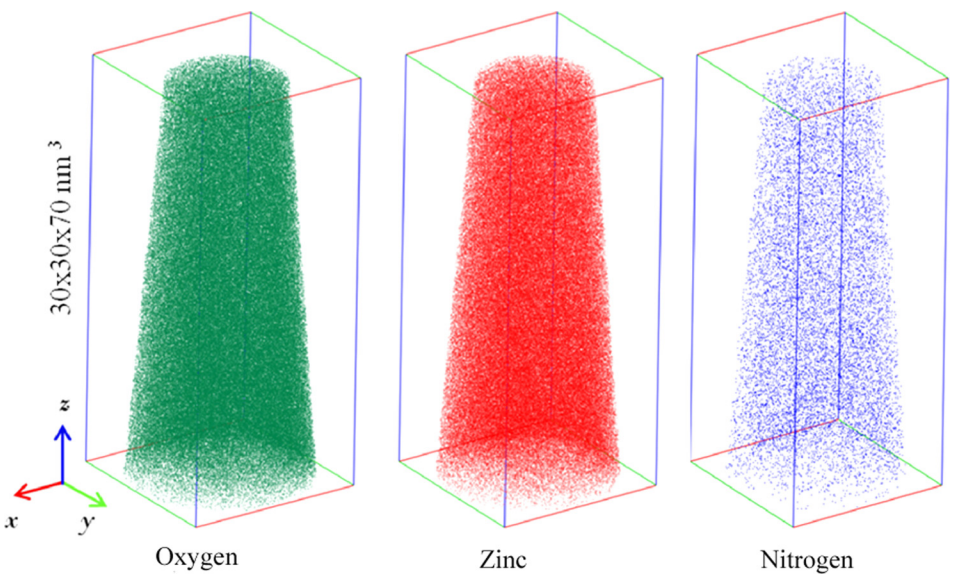

FIG. 9. 3D reconstruction of single N-doped ZnO nanowire obtained by APT. Oxygen, zinc, and nitrogen atoms are represented in green, red, and blue, respectively.

optimal condition is also appropriate to measure the dopant concentration. Note that for Eu-doped ZnO thin film, EDX measurements show a Eu concentration ($5.5\% \pm 1\%$) very close to the APT value (6%). It seems to confirm our postulate. Unfortunately, in our knowledge, for N-doped ZnO nanowires, no experimental technique is able to measure precisely the N content in such single nano-object.

Nevertheless, it shows that Zn^{2+}/Zn^{+} metric allows to perform reproducible experiments and should allow to follow the evolution of dopant concentration in a study of a series of nanowires grown at different dopant content.

The experimental results reported here show that, although there are challenges on APT of ZnO materials, proper field evaporation can be carried out by adjusting the operating parameters in order to obtain an optimum surface electric field, which can be accessed via the Zn^{2+}/Zn^{+} ratio. We suggest that such fundamental studies can be also applied for other semiconducting materials where the electronegativity of the cations and anions are close to the one on Zn and O, respectively. This fundamental study can help the atom probe and materials science community to perform a more reliable measurement and to harvest all the advantages that atom probe tomography technique can offer.

ACKNOWLEDGMENTS

The authors thank the French National Agency for the financial support (Project No. MADFIZ ANR-11-NANO-0013) and through the program "Investissements d'avenir" (ANR-10-LABEX-09-01), LABEX EMC3. François Vurpillot is warmly acknowledged for the fruitful discussion.

[1]D. C. Look, Mater. Sci. Eng. B **80**, 383 (2001).
[2]Ü. Özgür, Y. I. Alivov, C. Liu, A. Teke, M. A. Reshchikov, S. Doğan, V. Avrutin, S.-J. Cho, and H. Morkoç, J. Appl. Phys. **98**, 041301 (2005).
[3]A. Tsukazaki, A. Ohtomo, T. Onuma, M. Ohtani, T. Makino, M. Sumiya, K. Ohtani, S. F. Chichibu, S. Fuke, Y. Segawa, H. Ohno, H. Koinuma, and M. Kawasaki, Nat. Mater. **4**, 42 (2005).
[4]J. C. Sun, H. W. Liang, J. Z. Zhao, J. M. Bian, Q. J. Feng, L. Z. Hu, H. Q. Zhang, X. P. Liang, Y. M. Luo, and G. T. Du, Chem. Phys. Lett. **460**, 548 (2008).
[5]X. W. Sun, B. Ling, J. L. Zhao, S. T. Tan, Y. Yang, Y. Q. Shen, Z. L. Dong, and X. C. Li, Appl. Phys. Lett. **95**, 133124 (2009).
[6]C. H. Park, S. B. Zhang, and S.-H. Wei, Phys. Rev. B **66**, 073202 (2002).
[7]U. V. Desnica, Prog. Cryst. Growth Charact. Mater. **36**, 291 (1998).
[8]M. Naouar, I. Ka, M. Gaidi, H. Alawadhi, B. Bessais, and M. A. E. Khakani, Mater. Res. Bull. **57**, 47 (2014).
[9]A. Marzouki, F. Falyouni, N. Haneche, A. Lusson, P. Galtier, L. Rigutti, G. Jacopin, M. Tchernycheva, M. Oueslati, and V. Sallet, Mater. Lett. **64**, 2112 (2010).
[10]A. Souissi, N. Haneche, A. Meftah, C. Sartel, C. Vilar, A. Lusson, P. Galtier, V. Sallet, and M. Oueslati, J. Lumin. **136**, 265 (2013).
[11]J.-C. G. Bünzli and C. Piguet, Chem. Soc. Rev. **34**, 1048 (2005).
[12]V. Kumar, V. Kumar, S. Som, M. M. Duvenhage, O. M. Ntwaeaborwa, and H. C. Swart, Appl. Surf. Sci. **308**, 419 (2014).
[13]A. Cetin, R. Kibar, S. Selvi, P. D. Townsend, and N. Can, Phys. B Condens. Matter **404**, 3379 (2009).
[14]B. Gault, F. Vurpillot, A. Vella, M. Gilbert, A. Menand, D. Blavette, and B. Deconihout, Rev. Sci. Instrum. **77**, 043705 (2006).
[15]R. Lardé, L. Lechevallier, A. Zarefy, A. Bostel, J. Juraszek, J. M. L. Breton, B. Rodmacq, and B. Dieny, J. Appl. Phys. **105**, 084307 (2009).
[16]K. Inoue, F. Yano, A. Nishida, H. Takamizawa, T. Tsunomura, Y. Nagai, and M. Hasegawa, Ultramicroscopy **109**, 1479 (2009).
[17]M. Roussel, W. Chen, E. Talbot, R. Lardé, E. Cadel, F. Gourbilleau, B. Grandidier, D. Stiévenard, and P. Pareige, Nanoscale Res. Lett. **6**, 271 (2011).
[18]M. Roussel, E. Talbot, C. Pareige, R. P. Nalini, F. Gourbilleau, and P. Pareige, Appl. Phys. Lett. **103**, 203109 (2013).
[19]R. Lardé, E. Talbot, P. Pareige, H. Bieber, G. Schmerber, S. Colis, V. Pierron-Bohnes, and A. Dinia, J. Am. Chem. Soc. **133**, 1451 (2011).
[20]M. K. Miller, A. Cerezo, M. G. Hetherington, and G. D. W. S. FRS, *Atom Probe Field Ion Microscopy*, Monographs on the Physics and Chemistry of Materials 52 (Clarendon Press, 1996).
[21]D. Santhanagopalan, D. K. Schreiber, D. E. Perea, R. L. Martens, Y. Janssen, P. Khalifah, and Y. S. Meng, Ultramicroscopy **148**, 57 (2015).
[22]A. Devaraj, R. Colby, W. P. Hess, D. E. Perea, and S. Thevuthasan, J. Phys. Chem. Lett. **4**, 993 (2013).
[23]R. Kirchhofer, M. C. Teague, and B. P. Gorman, J. Nucl. Mater. **436**, 23 (2013).
[24]L. Mancini, N. Amirifar, D. Shinde, I. Blum, M. Gilbert, A. Vella, F. Vurpillot, W. Lefebvre, R. Lardé, E. Talbot, P. Pareige, X. Portier, A. Ziani, C. Davesnne, C. Durand, J. Eymery, R. Butte, J.-F. Carlin, N. Grandjean, and L. Rigutti, J. Phys. Chem. C **118**, 24136 (2014).
[25]D. R. Diercks, B. P. Gorman, R. Kirchhofer, N. Sanford, K. Bertness, and M. Brubaker, J. Appl. Phys. **114**, 184903 (2013).
[26]J. R. Riley, R. A. Bernal, Q. Li, H. D. Espinosa, G. T. Wang, and L. J. Lauhon, ACS Nano **6**, 3898 (2012).
[27]Y. M. Chen, T. Ohkubo, and K. Hono, Ultramicroscopy **111**, 562 (2011).
[28]N. Dawahre, G. Shen, S. Balci, W. Baughman, D. S. Wilbert, N. Harris, L. Butler, R. Martens, S. M. Kim, and P. Kung, J. Electron. Mater. **41**, 801 (2012).
[29]E. P. Silaeva, L. Arnoldi, M. L. Karahka, B. Deconihout, A. Menand, H. J. Kreuzer, and A. Vella, Nano Lett. **14**, 6066 (2014).
[30]K. Thompson, D. Lawrence, D. J. Larson, J. D. Olson, T. F. Kelly, and B. Gorman, Ultramicroscopy **107**, 131 (2007).
[31]M. Bachhav, R. Danoix, F. Danoix, B. Hannoyer, S. Ogale, and F. Vurpillot, Ultramicroscopy **111**, 584 (2011).
[32]S. Duguay, M. Ngamo, P. F. Fazzini, F. Cristiano, K. Daoud, and P. Pareige, Thin Solid Films **518**, 2398 (2010).
[33]M. Ngamo, S. Duguay, P. Pichler, K. Daoud, and P. Pareige, Thin Solid Films **518**, 2402 (2010).
[34]T. Kinno, M. Tomita, T. Ohkubo, S. Takeno, and K. Hono, Appl. Surf. Sci. **290**, 194 (2014).
[35]D. R. Kingham, Surf. Sci. **116**, 273 (1982).
[36]B. Gault, M. P. Moody, J. M. Cairney, and S. P. Ringer, *Atom Probe Microscopy*, 2012 ed. (Springer, New York, 2012).
[37]A. L. Allred, J. Inorg. Nucl. Chem. **17**, 215 (1961).
[38]Y. Xia, M. Karahka, and H. J. Kruzer, J. Appl. Phys. **118**, 025901 (2015).